Review of Lining Materials and Their Degradation in Aluminium Electrolysis Cells

Samuel Senanu[1], Egil Skybakmoen[2], Arne Petter Ratvik[3], Zhaohui Wang[4]
and Asbjørn Solheim[5]
1, 3. Senior Research Scientists
2. Research Manager
4. Research Scientist
5. Chief Scientist
SINTEF Industry, Trondheim, Norway
Corresponding author: samuel.senanu@sintef.no
https://doi.org/10.71659/icsoba2025-al076

Abstract

The need for high energy efficiency and productivity in modern high-amperage aluminium electrolysis cells gives extreme requirements to the lining materials used in the cells. The sidelining materials need high thermal conductivity, e. g., nitride-bonded silicon carbide blocks have replaced carbon side blocks. They are also thinner to accommodate wider anodes. In addition, the traditional coal tar pitch binder in the ramming paste has been replaced by the so-called eco-friendly and PAH-free binders. At the cathode, the collector bars are currently constructed with copper inserts or even as full copper bars. There is a tendency to use highly graphitised carbon cathode blocks to reduce energy consumption and maintain thermal balance at higher amperages. The high current densities that may result from the high amperages may facilitate the chemical reactions leading to the degradation of lining materials due to the increased activity of sodium. This review paper will attempt to give an overview of the current knowledge about the lining materials and their degradation mechanisms, as reported in the literature.

Keywords: High-amperage cells, Lining materials, Copper collector bars, Graphite cathode blocks, Degradation.

1. Introduction

Aluminium is currently the most produced non-ferrous metal in the world, with annual global production reaching approximately 73 million tonnes in 2024 [1]. The high production volume of aluminium is due to its numerous applications in modern society, owing to important properties that it possesses, such as corrosion resistance, light weight, excellent thermal and electrical conductivities, and the ability to be alloyed with other metals, etc. The production of aluminium occurs through the Hall-Héroult process, which is based on the electrochemical reduction of aluminium oxide in an electrolysis cell at about 960 °C to 970 °C [2]. The electrolysis cell for producing aluminium consists of carbon anodes that conduct electricity as well as heat and are consumed during the production process, a fluoride melt consisting mainly of cryolite that conducts electricity and dissolves alumina, an aluminium metal pad that acts as the electrochemical cathode, a cathode lining consisting of carbon cathode blocks (with different degrees of graphitisation) rodded with collector bars for conducting electricity and ramming paste to fill the joints between the cathode blocks, a refractory lining, insulation materials, and a side wall material. The carbon cathode lining, the refractories, insulations, and side wall materials are usually arranged in a rectangular steel shell that varies from 9 to 18 m long, 3 to 5 m wide and 1 to 1.5 m deep [2]. The operating cavity depth after installation of all lining materials is about 0.4 to 0.5 m [2]. The molten electrolyte and aluminium metal pad are usually kept at a height of 15–20 cm and 10–20 cm, respectively, during the electrolysis process [2, 3]. There are two types of technologies that are based on the design of the carbon anode: prebaked and Søderberg technologies [2, 4]. Figure 1 is a sketch of the electrochemical reduction cell using the prebaked anode technology.

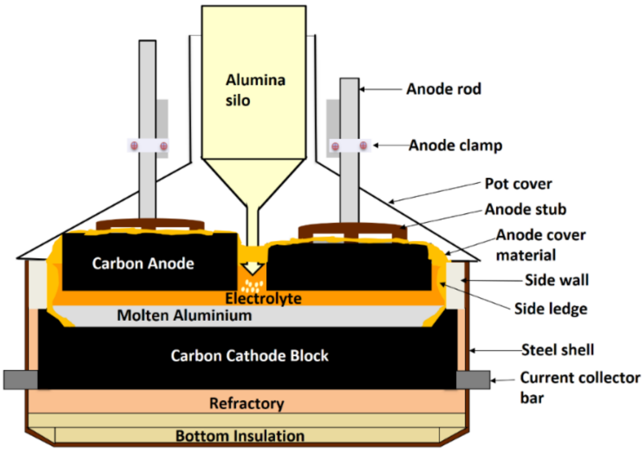

Figure 1. Electrochemical reduction cell using prebaked anode technology [5].

The lining materials within the electrolysis cell will, over time, degrade or, in some extreme conditions, fail, leading to the shutdown of the cell [6]. The time from when an electrolysis cell is started to when it must be decommissioned is referred to as the pot age. The pot age varies a lot and can be from a few hundred days to over 3000 days [7, 8]. The physical and chemical stability of the lining materials varies over time in the electrolysis cell and plays a crucial role in the degradation of the cell lining and consequently the pot life. Owing to the high financial costs relating to building a new cathode lining, loss in production, and disposal of the spent pot lining material after the curtailment, it is imperative to understand the degradation mechanism(s) of the lining materials. This paper presents a review of the different lining materials currently in use in the aluminium electrolysis cells and their degradation mechanism(s).

2. Cathode Lining Materials

2.1 Carbon Cathode Blocks

The use of carbon cathode blocks by the aluminium industry in the construction of the electrolysis cell is due to important properties such as high thermal and electrical conductivity, stability towards molten cryolite and aluminium, mechanical strength, etc. [9]. The carbon cathode blocks used in the aluminium industry are grouped or classified into three main categories, namely graphitised cathode blocks, graphitic cathode blocks and amorphous cathode blocks. The graphitised cathode blocks consist of a graphitizable material (petroleum coke) and binder (coal tar pitch) that have been heat-treated to temperatures reaching 3000 °C, thereby graphitising the whole material. Thus, the graphitised cathode blocks have both the filler and binder content fully graphitised. Some manufacturers impregnate their cathode blocks with pitch before graphitisation to reduce open porosity. Graphitic cathode blocks are made from graphitizable materials such as petroleum coke and/or scrap graphite aggregates, and a coal tar pitch binder. However, the heat treatment is up to ca. 1200 °C, and thus the cathode block is not graphitised as in the case of the graphitised cathode blocks. Amorphous cathode blocks consist of gas or electrocalcined anthracite and a coal tar pitch binder that has been heated to ca. 1200 °C [9]. The high temperature treatment of the filler and binder content of the carbon cathode blocks leads to a higher degree of crystallinity, which is favourable for important properties such as electrical resistivity, especially at temperatures of 2000 °C and above [10]. Table 1 gives some of the important properties of the carbon cathode blocks currently in use in the aluminium industry.

Table 1. Important properties of carbon cathode materials used in the aluminium industry. Reproduced from Sørlie and Øye [3].

Property	Amorphous			Graphitic	Graphitised
Filler Material:					
Anthracite, %	100	70–80	50	-	-
Graphite, %	-	20–30	50	100	-
Petroleum coke, %	-	-	-	-	100
Real density, g/cm^3	1.84–1.88	1.85–1.93	1.90–1.95	2.00–2.16	2.18–2.2
Bulk density, g/cm^3	1.52–1.58	1.53–1.60	1.57–1.61	1.60–1.66	1.57–1.68
Total porosity, %	15–19	15–19	17–21	20–24	24–28
Open porosity, %	13–16	15–16	16–17	18–20	20–24
Specific electrical resistance, µΩ·m	36–55	29–44	25–34	15–24	10–15
Thermal conductivity, W/m·K	6–14	8–15	12–27	20–45	100–140
Linear thermal expansion. coefficient, µm/m·K	2.2–2.6	2.2–2.6	2.2–2.6	1.9–2.6	1.8–3.6
Crushing strength, MPa	18–33	18–32	19–33	19–34	18–27
Bending strength, MPa	6–8	6–10	7–10	8–10	6–12
Ash content, %	4–6	3–6	2–4	0.5–1.3	0.1–0.6
Sodium expansion, %	0.5–1.3	0.3–1.0	0.2–0.7	0.1–0.4	< 0.1–0.8
Thermal shock resistance	1	1.5	2.5	3.5	25
Abrasion index (relative to 100 % amorphous)	1	2	4	4	200

The aluminium industry over the past decades has gradually migrated from the amorphous and graphitic cathode blocks to the more graphitised cathode blocks. This is due to the high thermal and electrical conductivity of graphitised cathode blocks, which helps to obtain higher energy efficiency and productivity. The high thermal conductivity helps to maintain the thermal balance of the electrolysis cells as the industry creeps to higher amperages [11]. Despite the excellent electrical and thermal conductivities, the literature reports of uneven current distribution over the cathode surface, with the current peaking at the ends of graphitised cathode blocks [9, 12].

2.2 Cathode Collector Bars

The current flowing through the electrolysis cell is conducted out of the cell via collector bars rodded into the carbon cathode blocks. These cathode collector bars are usually sealed to the carbon cathode blocks using cast iron, carbon ramming paste, carbonaceous glues or cement [9]. The cathode collector bars have traditionally been made of steel, with cast iron as the common material for sealing. However, just like the transition from the less graphitised (graphitic and amorphous) cathode blocks to the more graphitised blocks to improve energy efficiency and productivity, the collector bars have also seen a transition. For a better current distribution over the length of the carbon cathode blocks and reduced cathode voltage drop, the industry is currently moving from having only steel cathode collector bars to highly electrically conducting copper as a copper insert into the steel collector bars or having a full copper collector bar [9, 13, 14].

2.3 Carbon Ramming Paste

The carbon ramming paste plays a crucial role in sealing all gaps or voids between the carbon cathode blocks and the cathode periphery to prevent liquid metal and bath from rapidly penetrating the inner parts of the cathode lining. It also acts as a cushion to absorb some of the thermal expansion of the carbon cathode blocks during preheating of the cathode lining. Ramming paste consists of filler and binder components. The filler component is traditionally amorphous carbon, comprising mostly of anthracite, whereas the binder component is coal tar pitch [9].

However, due to the need to spill more heat in high-amperage electrolysis cells, some or all of the amorphous content has been replaced with high-conducting carbon materials such as synthetic graphite [9]. Also, strict health and environmental regulations have seen manufacturers replacing the traditional coal tar pitch binder with synthetic organic binders/resins in their products. These ramming paste materials with different binders are given names such as "eco-friendly" or "environmentally friendly" or PAH-free ramming pastes. This is to reduce the content of polycyclic aromatic hydrocarbons (PAH) in their products [9, 15, 16]. The thermo-mechanical behaviours of these pastes during baking have been observed to differ from their traditional counterparts or each other in some cases [16].

Two types of ramming paste exist in the aluminium industry: hot and tepid or cold ramming pastes [9]. The hot ramming requires pre-heating to temperatures of ca. 100 °C before installation during the cathode construction. The pre-heating may enhance the fluidity and adhesion of the material to the cathode blocks, however, the requirement for heating implies the operation needs to be done quickly to avoid lamination, which would occur if the first layer cools before the next hot mix of ramming paste material is applied. It might also be necessary to preheat the cathode blocks before ramming with hot ramming pastes in cold countries, which might increase the total installation cost due to the additional energy and equipment required. Furthermore, the hot ramming operation poses challenges relating to the safety and health of the workers due to heat and exposure to tar fumes and PAH. Due to the challenges relating to the health, safety and quality of the ramming operation, the hot ramming paste is limited to very few smelters across the industry [9].

Table 2. The two types of ramming paste with and without coal tar pitch binders. Reproduced from [9, 15].

Property	**Hot ramming paste**	**Cold or tepid ramming paste**			
Filler material	Anthracite	Anthracite	Graphite	Anthracite	Anthracite
Binder material	Coal tar pitch	Coal tar pitch	Coal tar pitch	PAH-free binder	Eco friendly
Green properties					
Temperature window, °C	140–180	10–50	10–50	10–50	10–50
Bulk density, g/dm^3	1500–1600	1500–1600	1550–1750		
Baked properties					
Real density, g/dm^3	1800–1900	1800–1900	2000–2200	-	-
Bulk density, g/dm^3	1400–1600	1400–1500	1300–1650	1381–1431	1450–1468
Porosity, %	15–25	15–30	20–40	18.8–22.6	18.3–19.1
Crushing strength, MPa	25–40	15–40	5–25	17.4–18.2	12.7–15.6
Electrical resistivity, μΩ·m	60–80	60–90	30–60	48.6–70.4	70–92
Ash content, %	4–10	4–10	0.5–2	2.3–3.3	2.9–6.6

The cold or tepid ramming paste, also called room temperature ramming pastes, is the dominant ramming paste currently in use in the aluminium industry. This ramming paste type eliminates the challenges with health, safety, the need for additional equipment and energy, etc. However, to make these paste types rammable at room temperature, the coal tar pitch binder is mixed with suitable softeners or solvents to lower the softening points. The solvent vaporises early in baking without the formation of a binder coke, which results in a relatively low-density, high porosity binder matrix. Also, the cold ramming paste has a limited shelf life due to evaporation of solvents or polymerisation. It is thus very important to ensure that the paste has not deteriorated before usage [9]. Nevertheless, once the cold ramming paste has been rammed in place in the constructed cathode lining, the storage life is considerably extended. However, a partly rammed cathode lining should not be stored with the ramming surface exposed to air for longer periods, as it will dry out and not bond to a paste applied later [9]. Table 2 is a summary of the important properties of the two types of ramming paste in use in the aluminium industry, including data on PAH-free and eco-friendly binders.

2.4 Side-Lining Materials

The side-lining materials used in the construction of the aluminium electrolysis cell are carbon and silicon carbide blocks due to their excellent thermal conductivities, which is a prerequisite for forming the much-needed side ledge, and their stability in molten cryolite and aluminium. Additionally, these side lining materials are expected to be resistant to oxidation, especially at the upper part above the bath [9, 17]. Carbon blocks have been replaced by nitride-bonded silicon carbide blocks either at the upper section of the sidewall or the whole sidewall in modern high amperage electrolysis cells over time due to their excellent oxidation resistance relative to carbon, stability in molten cryolite and metal, and high thermal conductivity. These materials consist of SiC and Si grains mixed with an organic binder. The silicon nitride binder is formed during the nitration stage of the production process [9, 18, 19]. Self-bonded silicon carbide, SiC, is another SiC-based sidelining material currently being tested for use in industry. This material is assumed to be superior to the nitride-bonded silicon carbide materials. It is reported that the thermal conductivity of SiC is about half that of graphite, which provides the opportunity to reduce its thickness by half to obtain a similar thermal conductivity. This allows for more room in the cell for longer carbon anodes and higher metal production capacity.

2.5 Refractory Lining

The refractory lining is usually placed beneath the carbon cathode blocks in the electrolysis cells, and it generally consists of refractory bricks and refractory aggregates normally used as levelling materials for the carbon cathode blocks. Aside from acting as a solid base for the carbon cathode blocks, the refractory layer's main function is to protect the bottom insulation from the infiltration of bath components and maintain the thermal balance [9, 20]. Traditionally, refractory bricks used in the aluminium industry have consisted of aluminosilicate, anorthite, and olivine-based refractory materials [9]. However, over the years, aluminosilicate refractory materials have proven to be the material of choice due to important considerations relating to stability, cost, and formation of favourable penetration barriers like albite as in the case of the chamotte-type refractory bricks with high silica content and low alumina content [9, 17, 20, 21]. Some properties of the chamotte-type refractories are given in Table 2 below.

Table 2. Important properties of chamotte bricks used for aluminium electrolysis [9, 17].

Property	Value
Bulk density, g/cm^3	2.10–2.20
Open porosity, %	19–23
Cold crushing strength, MPa	25–30
Thermal conductivity, W/m·K	
at 300 °C	1.20
at 600 °C	1.38
at 900 °C	1.45
Cryolite resistance, cm^2	< 5
Chemical composition, wt%	
Al_2O_3	32–44
SiO_2	52–64
Fe_2O_3	1.5–1.9
TiO_2	1.7
CaO + MgO	0.6
$Na_2O + K_2O$	1.2–2

2.6 Insulation Materials

The bottom insulation materials play the crucial role of conserving energy and thermal balance within the aluminium electrolysis cell. This is crucial to prevent the freezing of cryolite onto the carbon cathode blocks and to reduce the energy consumption of the process [4, 9]. The insulation materials used in the aluminium electrolysis cells are usually made up of diatomaceous earth bricks, also called Moler bricks, calcium silicate boards and vermiculite insulation boards. The low thermal conductivity of these materials is brought about by their very high open porosity filled with air. The insulating property is provided by still air found in these open porosities. Another group of insulation materials with insulation properties better than still air is microporous insulation materials. The super-insulating properties of these materials arise from the microscopic voids created by the ceramic particles and fibres within fumed silica, which minimises all three modes of heat transfer, namely, convection, conduction and radiation [9]. Table 3 summarises some of the properties of the insulation materials.

Table 3. Properties of different brands of insulation materials. data from Skamol AS.

Properties	**SkamoAlu V-1100 (375) Vermiculite**	**SkamoAlu VIP 12 Vermiculite**	**SkamoAlu Hiporos Moler**	**SkamoAlu Supra Moler**	**SkamoAlu S-1100E CaSi**	**SkamoAlu MP-1000 Microporous**
Density, kg/m^3	375	1200	570	750	245	280
Max. service temperature, °C	1100	1100	900	950	1100	1000
Porosity, %	85	56	76	68	90	-
CCS, MPa	1.3	9.5	1.6	7.5	2.7	0.33
Thermal conductivity, W/m·K						
at 200 °C	0.12	0.25	0.12	0.15	0.08	0.023
at 400 °C	0.15	0.27	0.14	0.17	0.10	0.026
at 600 °C	0.16	0.29	0.16	0.19	0.12	0.030
at 800 °C	0.19	0.30	0.18	0.21	0.14	0.036
Chemical composition, %						
SiO_2	46	52	72	77	47	-
Al_2O_3	7.0	23	8.0	9.0	0.3	-
CaO	3.5	1.5	6.5	0.8	43	-
MgO	19	8.9	1.2	1.3	0.6	-

3. Degradation of Cathode Lining Materials

The degradation of the cathode lining materials is facilitated by the presence of sodium, bath components, air and process gases such as hydrogen fluoride, HF, CO, CO_2, sulphur-containing gases including SO_2 and SO_3, etc. It is widely agreed in the industry that sodium paves the way for bath infiltration into the cathode lining and the consequent degradation by the infiltrating components [9, 22].

3.1 Carbon Cathode Blocks

Degradation of the carbon cathode blocks is reported to occur via three main mechanisms based on autopsy and laboratory investigations. These are physical or mechanical wear, chemical wear and electrochemical wear [5, 9, 22–26].

The physical or mechanical wear results mostly from cell operation activities such as cavity cleaning during anode change and metal tapping. It is also reported that the movement of alumina particles on the cathode surface contributes to physical wear because of their abrasive nature [9, 25, 26]. Laboratory investigation to determine abrasive resistance of different types of carbon cathode due to its importance to physical or mechanical wear resulted in the ranking: Graphite ≈ Graphitised < Graphitic < Anthracitic. The ranking suggests a higher abrasive resistance for the amorphous carbon materials relative to the less amorphous carbons. Wilkening and Reny also showed from their measurements that graphite cathode blocks have inferior erosion resistance [27]. However, Tschöpe found no significant differences between the wear rates of commercial cathode materials with different abrasion resistance [28]. The observation that different commercial cathode materials with different abrasion resistance showed similar wear rates may suggest that physical or mechanical wear is not the dominant wear mechanism, but rather chemical and/or electrochemical wear [9].

Chemical wear involves the formation, dissolution and transport of aluminium carbide, Al_4C_3, from the surface of the carbon cathode block [9]. The formation of aluminium carbide is expected to occur via a chemical reaction between carbon and aluminium, as is given by Equation (1), due to the thermodynamically favourable nature of the reaction (Gibbs energy of -147 kJ) at the electrolysis temperature of ca. 970 °C. However, laboratory investigations show a limited amount of carbide formation from the direct contact between carbon and aluminium at temperatures below 1000 °C [9, 26, 29, 30]. The low carbide formation is attributed to the poor wettability of molten aluminium towards carbon due to the presence of an oxide film around the aluminium [9, 29–32]. The presence of molten cryolite enhances the carbide formation as it dissolves the oxide film, thereby improving the wettability [9, 31]. Sodium plays a crucial role in the deterioration of lining materials, including the carbon cathode blocks. The formation of Na on the cathode surface is given by Equations (2) and (3). Another route for carbide formation is through the chemical reaction between the electrolyte and carbon in the presence of sodium, as shown by Equation (4). This reaction explains the presence of carbide within the carbon cathode lining during autopsy investigations.

$$4\,Al\,(l) + 3\,C(s) = Al_4C_3\,(s) \tag{1}$$

$$Na^+ + e^- = Na(in\,Al) \tag{2}$$

$$3\,NaF + Al\,(l) = 3Na + AlF_3\,(s) \tag{3}$$

$$4Na_3AlF_6(diss) + 12Na(in\,C) + 3C = Al_4C_3\,(s) + 24NaF(s) \tag{4}$$

Aside from the formation of aluminium carbide, another important factor for the chemical wear of carbon cathode lining is the dissolution and transport, as this ensures new surfaces are converted into carbide for the wear process to continue [9]. The dissolution of aluminium carbide in molten aluminium and cryolite suggests a two orders of magnitude higher for the dissolution in the molten cryolite [9, 29]. This suggests the molten cryolite plays a dominant role in the wear of the carbon cathode lining than the molten aluminium. Furthermore, it has been reported by Ødegård et. al. [33] that high temperature and acidic bath lead to higher dissolution of the carbide layer which results in a higher wear of the carbon cathode lining. Once dissolved in molten cryolite, aluminium carbide gets transported from the cathode surface due to convective patterns set up by the magnetic field within the metal pads. This movement allows the molten cryolite with the dissolved carbide to be replaced with fresh bath continuing the wear process [9, 34]. The carbide dissolution reaction reported by Ødegård et. al. [33] is represented by Equation (5).

$$Al_4C_3(s) + 5AlF_3(diss) + 9NaF(diss) = 3Na_3Al_3CF_8\,(diss) \tag{5}$$

Electrochemical wear of the carbon cathode lining also involves aluminium carbide formation, dissolution and transport, which is influenced by current density. Thus, the wear rate is directly related to the current density on the cathode surface. The carbide formation is reported to result from electrochemical reactions occurring on the cathode surface due to the more negative potentials existing on the cathode block and the ohmic voltage drop created across the penetrating bath and sludge [35]. The presence of electrolyte on the cathode surface results in the electrochemical reactions illustrated by the anodic and cathodic half-reactions given by Equations (6) and (7).

$$Anodic: \quad 4Al(l) + 12F^- = 4AlF_3(diss) + 12e^- \tag{6}$$

$$Cathodic: \quad 3C(s) + 4AlF_3(diss) + 12e^- = Al_4C_3(s) + 12F^- \tag{7}$$

Several researchers have reported the influence of current density distribution on the cathode surface and bath chemistry on the wear of the carbon cathode [27, 36–40]. Gudbrandsen et. al. [40] observed an increased electrochemical wear with a corresponding increase in cathodic current density up until a limiting current. However, this dependency of electrochemical wear on the current density was further studied by Wang et. al. [41] who discovered a further increase in the cathode wear upon increasing the current density above 1 A/cm². This further increase was attributed to increased sodium activity at the higher current densities, leading to increased carbide formation and the consequent increased electrochemical wear.

3.2 Cathode Collector Bars

The cathode collector bars undergo different deterioration mechanisms during the operation of the electrolysis cell. Aside from the high temperature creep that the collector bars experience due to the proximity to the carbon cathode blocks, they are exposed to penetrating bath components, metal, sodium vapour, and reaction products from the underlying refractory lining and the pressure created by these reactions [9]. The high temperature creep reduces the yield strength of the bars, whereas the exposure to metal and bath components alters the chemical composition. Analysis of collector bar samples collected during autopsies has been reported to include Fe-Al and FeSi alloys [9]. The introduction of copper inserts, as well as full copper cathode collector bars, introduces other reaction components such as Fe-Cu and Al-Cu alloys [13, 14]. The formation of Fe-Cu alloys is reported to originate from the diffusion of iron into the copper insert during operation. The formation of Al-Cu (aluminium bronze) alloys from full copper cathode collector bars is reported to originate not only from the direct contact with infiltrated aluminium metal, but rather aluminium from reduced electrolyte due to the presence of Na, as is given by Equation (8) [13, 14].

$$\frac{1}{3}Na_3AlF_6(s) + 12Na(g) = \frac{1}{3}Al\ (l) + 2NaF(s) \tag{8}$$

The formation of the different alloys mentioned in this section leads to changes in the cathode collector bars that decrease the electrical conductivity, contributing to higher cathode voltage drops, reducing the mechanical strength, leading to early failures, volume expansions that result in cracking of the carbon cathode blocks, etc. [9, 13, 14].

3.3 Carbon Ramming Paste

The carbon ramming paste also undergoes the degradation mechanisms of carbon cathode blocks, such as physical or mechanical wear, chemical and electrochemical wear induced by aluminium carbide formation. However, considering the importance of the carbon ramming paste in sealing all gaps between cathode blocks and other spaces as well as accommodating the thermal expansion of the cathode blocks, its physical properties such as shrinkage, densification, mechanical strength and thermo-plastic behaviour during preheating and later cell operation play a deciding factor in the failure of the whole cathode lining. It is reported that over-compaction leads to crushing of the aggregate, which leads to poor mechanical strength and stratification [42]. Also, the relatively high porosity of the ramming paste relative to the carbon cathode blocks implies extensive infiltration of the bath, as well as metal and aluminium carbide formation within the porosity if the ramming operation is not carried out properly [9]. The relatively low electrical conductivity of the ramming paste suggests a lower electrochemical wear mechanism relative to the carbon cathode blocks, which is visible in the ramming joint being less worn out than the rest of the cathode block [5, 9].

3.4 Si_3N_4-Bonded SiC Side-Lining Materials

The degradation mechanisms of nitride-bonded silicon carbide sidewall materials are generally divided according to their location on the sidewall, also referred to as zones [9, 43, 44]. These zones are the gas zone (above the electrolyte level up to the deck plate), the bath zone (between the electrolyte and metal levels) and the metal zone (below the electrolyte level). Each of these zones presents a different chemical environment that influences the degradation reactions occurring. The reactions occurring in these zones, as reported in the literature, are summarised below.

Gas zone: The chemical components reported for the gas zone include $NaAlF_4$ (g), H_2O (g), HF, SiF_4, Na (g), CO, CO_2, O_2 [43, 44]. The relative stability of nitride-bonded silicon carbide sidewall materials relative to the carbon sidewall materials is due to the formation of a passive layer of SiO_2 when in contact with O_2. However, this passive layer is easily attacked by the cryolite melt when exposed to it. Furthermore, the components of the sidewall material, Si_3N_4 and SiC, are both unstable in NaAlF4 (g) and CO_2 and may react to form the components $NaAlSiO_4$ and SiF_4 (g). Moreover, Na (g) and HF could also react with the components to form Na_2SiO_3 and SiF_4, respectively, leading to the degradation of the material [44]. The Si_3N_4 binder is reported to be the weakest part of the sidewall material as it presents a larger surface area relative to SiC for reaction and degradation. Porosity of the sidewall material is reported to play a very important role in the degradation mechanisms occurring in the gas zone due to access to large internal surfaces for oxidation and consequent degradation [45]. It is reported that the most severe degradation of the sidewall material occurs at the gas/bath interface [43].

Bath zone: The presence of sodium, together with gases indicative of the electrolysis process, plays an important role in the degradation of sidewall material located in the bath zone. Tests done in the laboratory by Skybakmoen et al. [46] showed that Si_3N_4-bonded SiC blocks did not corrode when exposed to molten aluminium and cryolite at 1000 °C for 720 h in argon atmosphere without electrolysis. Also, investigation of autopsy samples showed that the main reaction products of the sidewall materials located here were Na_2SiO_3 and $Na_2Si_2O_5$, which are indicative of reactions with sodium and electrolysis process gases like CO and CO_2 [44].

Metal zone: The main reaction product reported for this zone includes Al_4C_3, Si metal and AlN, suggesting a reaction between the sidewall material and the molten aluminium metal.

3.5 Refractory Lining

Degradation of the refractory lining is reported to start with chemical reactions initiated by the presence of sodium. The presence of sodium opens the path for the infiltration of fluorides from the penetrating electrolyte [9, 22]. Infiltration of fluorides leads to reactions with the refractory lining, causing mineralogical changes in the refractory [21, 47]. For the aluminosilicate bricks that are traditionally employed in the aluminium electrolysis cells, sodium will reduce both the alumina and silica contents of the refractory in addition to the reaction products between the penetrating fluorides and refractory material. Some of the reactions involving the infiltrating fluorides and sodium are given in Equations (9) to (12) below.

$$2Al_2O_3(s) + 3SiO_2(s) + 6NaF(l) = 3NaAlSiO_4(s) + Na_3AlF_6 \tag{9}$$

$$2Al_2O_3(s) + 9SiO_2(s) + 6NaF(l) = 3NaAlSi_3O_8(s) + Na_3AlF_6 \tag{10}$$

$$\frac{3}{8}NaAlSi_3O_8(s) + Na(g) = \frac{3}{8}NaAlSiO_4(s) + \frac{1}{2}Na_2SiO_3(s) + \frac{1}{4}Si(s) \tag{11}$$

$$\frac{3}{4}NaAlSiO_4(s) + Na(g) = \frac{3}{4}NaAlO_2(s) + \frac{1}{2}Na_2SiO_3(s) + Si(s) \tag{12}$$

Equations (9) and (10) show the first reaction products formed after fluoride attack on the aluminosilicates. It is reported that the reaction product given in Equation (10) also called albite is a glassy phased material with the ability to retard the degradation mechanisms and thus preferred over the reaction product given by Equation (9) also called nepheline. As can be seen from the reaction, a higher SiO_2 content is necessary for the formation of the albite phase, and thus, the industry goes for aluminosilicate bricks with a higher SiO_2 content as discussed in the sections above. Despite the importance of albite in retarding the degradation mechanism it can be seen from Equation 11 that it is reduced by sodium to nepheline thereby losing its glassy barrier properties [9]. Due to the reducing nature of sodium vapour, some smelters employ physical barriers such as steel plates, graphite foil and glass on top of the insulation lining to reduce the passage of sodium vapour [9].

Aside from the degradation of refractories due to sodium and infiltrating fluorides, liquid aluminium is reported to cause severe degradation of the refractory lining if it penetrates the lining due to cracks or failures in the lining. The very severe degradation is due to the very exothermic reactions between the molten metal and the silica content of the refractory materials at the electrolysis operating temperatures [9]. Equation (13) illustrates this reaction.

$$3SiO_2(s) + 4Al(l) = 3Si(s) + 2Al_2O_3(s) \tag{13}$$

The reaction mechanisms for the anorthite refractories are given by Equations (14) and (15), whereas that of olivine refractories is given by Equation (16) as follows.

$$CaAl_2Si_2O_8(s) + 2NaF(l) = Na_2Al_2Si_2O_8(s) + CaF_2(s) \tag{14}$$

$$\begin{aligned} &6CaAl_2Si_2O_8(s) + 2Na_3AlF_6(l) = \\ &\qquad 6CaF_2(s) + 3NaAlSi_3O_8(l) + 3NaAlSiO_4(s) + 4Al_2O_3(s) \end{aligned} \tag{15}$$

$$Mg_2SiO_4(s) + Na_3AlF_6(l) = 2NaMgF_3(s) + NaAlSiO_4(s) \tag{16}$$

3.6 Insulation Materials

The relatively low density and high porosity of the insulation materials make them vulnerable to degradation by fluorides and gases found within the lining, as larger surface areas are made available for degradation reactions. For insulation materials with chemical components similar to those of the refractory lining, i. e. Al_2O_3 and SiO_2, the reactions given by Equations (9) to (13) will occur, however, to a higher degree because of the high porosity [9]. For the insulation lining, the reaction with molten aluminium, as shown by Equation (13), will lead to a complete conversion of the whole insulation lining if the refractory lining fails, especially during the early days of operation when the open porosity is free for reactions. Reaction products indicative of aluminothermic reactions, such as $FeAl_2$ and $FeAl_2Si$, have been observed in autopsy samples from the insulation lining, whereas in the worst-case scenario, the whole insulation lining has been replaced by aluminium metal [9]. Aside from the chemical degradation of the insulation lining, these materials are also exposed to high temperatures and compression from the lining materials on top of them. Insulation materials are reported to be dimensionally unstable, experience shrinkage and changes in crystalline structures at higher temperatures [9, 48, 49].

4. Conclusions

The literature studies have shown that extensive work has been done in understanding the cathode lining materials used in the aluminium industry in terms of material properties and degradation mechanisms. The studies reveal that sodium is by far the dominant factor in the degradation of the cathode lining as it partakes in the reduction of materials, including oxides within the refractory and insulation lining, etc. It also paves the way for electrolyte infiltration into the whole cathode lining, thereby kickstarting the fluoride attack of the refractories and insulation lining. Despite the dominant role of sodium in the degradation of the lining, the literature also reports the devastating degradation that occurs if the lining material fails to prevent the rapid infiltration of molten aluminium and cryolite due to cracks or imperfections created due to bad cathode construction procedures. The chemical components chosen for the refractories used in the aluminium electrolysis cells are designed to form effective penetration barriers like albite, to reduce the degradation rates, and thus, proper construction procedures may help to maintain acceptable pot life.

Moreover, the importance of electrochemical and chemical wear relative to physical or mechanical wear of the carbon cathode blocks suggests that a uniform current distribution and calm metal and bath movements are crucial to obtain a relatively uniform wear pattern along the cathode surface that could contribute to higher pot age even as amperages are increased. This is especially true for the highly electrically conducting graphitised cathode blocks due to the peaking of current at the ends of the cathode blocks. The use of copper insert collector bars as well as full copper collector bars may help to even out the current distribution along the cathode block; however, actions need to be taken to prevent the copper from contacting chemical components that could react with it and change its properties. Furthermore, it is crucial to test the lining materials used in the construction of cathode lining to ensure they meet the specifications provided by the suppliers before installing them, as properties such as porosity, density, mechanical and chemical stability play a very important role in determining the rate of the degradation mechanisms.

5. Acknowledgement

The authors wish to express profound gratitude to Dr Morten Sørlie and the late Emeritus Professor Harald A. Øye for their extensive and pioneering contributions to the understanding of cathode lining materials degradation in aluminium electrolysis cells. Their work has laid a critical foundation for ongoing research and advancement in cathode lining materials for the aluminium industry.

6. References

1. International Aluminium Institute website, https://international-aluminium.org/statistics/primary-aluminium-production/ (Accessed on 23 June 2025).
2. Jomar Thonstad et al., *Aluminium electrolysis: Fundamentals of the Hall-Héroult process*, Aluminium-Verlag Marketing and Kommunikation GmbH, 2001.

3. Halvor Kvande and Per Arne Drabløs, The aluminium smelting process and innovative alternative technologies, *Journal of Occupational & Environmental Medicine* 2014, 56, S23–S32. https://doi.org/10.1097/jom.0000000000000062
4. Kai Grjotheim and Harald Kvande, *Introduction to aluminium electrolysis: Understanding the Hall-Héroult process*, Aluminium-Verlag, 1993. https://doi.org/10.1007/978-1-4613-4136-9_23
5. Samuel Senanu, *Cathode Wear in Aluminium Electrolysis Cells*, PhD Thesis, Norwegian University of Science and Technology, 2019. http://hdl.handle.net/11250/2627792.
6. Morten Sørlie and Harald A. Oye, *Cathodes in aluminium electrolysis*, Aluminium-Verlag Marketing & Kommunikation GmbH, 2010.
7. Morten Sørlie, Jan Hvistendahl and Harald A. Øye, Early failure mechanisms in aluminium cell cathodes, *Light Metals* 1993, 299–308, also in *Essential Readings in Light Metals* 2016, 921-930. https://doi.org/10.1007/978-3-319-48200-2_122
8. Samuel Senanu et al., Cathode wear based on autopsy of a shutdown aluminium electrolysis cell, *Light Metals* 2017, 561–570. https://doi.org/10.1007/978-3-319-51541-0_70
9. Morten Sørlie and Harald A. Oye, *Cathodes in aluminium electrolysis*, Aluminium-Verlag Marketing & Kommunikation GmbH, 2010.
10. S. R. Brandtzæg, H. Linga and H. A. Øye, Structural changes in carbon by heat treatment, *Essential Readings in Light Metals* 2016, 754–761. https://doi.org/10.1007/978-3-319-48200-2_99
11. L. Rivoaland, Development of a New Type of Cathode for Aluminium Electrolysis, in: *Proceedings of the 34th International ICSOBA Conference*, 3-6 October 20216, Quebec City, Canada, 2016: *TRAVAUX* 45, 757–765.
12. J.M. Dreyfus and L. Joncourt, Erosion mechanisms in smelters equipped with graphite blocks - a mathematical modeling approach, *Light Metals* 1999, 199–206.
13. Oscar Alberto Vera Garcia1 et al., The robustness of ready-to-use cathodes (RuC®) - a mature technology available for the primary aluminium industry, *Proceedings of 42nd International ICSOBA Conference*, 27-31 October 2024, Lyon, France, *TRAVAUX* 53, 1633–1642. https://doi.org/10.71659/icsoba2024-al050
14. Nadia Ahli et al., EGA experience with full copper cathode collector bars, *Proceedings of 42nd International ICSOBA Conference*, 27-31 October 2024, Lyon, France, *TRAVAUX* 53, 1643-1656. https://doi.org/10.71659/icsoba2024-al051
15. Bénédicte Allard, Mohamed Tawfik and Arvind Kumar, Performances of green and eco-friendly ramming pastes in ega pots, *Metals* 2016, 6(5). https://doi.org/10.3390/met6050112
16. Alexander Arkhipov et al., EGA journey with different ramming pastes, *Light Metals* 2022, 911–920. https://doi.org/10.1007/978-3-030-92529-1_119
17. Andrey Yurkov, *Refractories for aluminium*, Springer International Publishing, 2015. https://doi.org/10.1007/978-3-319-11442-2
18. Egil Skybakmoen et al., Quality evaluation of nitride bonded silicon carbide sidelining materials, *Light Metals* 2005, 773–778. https://doi.org/10.1007/978-3-319-48200-2_114
19. Egil Skybakmoen, Quality evaluation of nitride–bonded sic sidelining materials: historical trends 1997–2022 including results and development of test methods, *Light Metals* 2022, 921–928. https://doi.org/10.1007/978-3-030-92529-1_120
20. Christian Schøning, Tor Grande and Ole-Jacob Siljan, Cathode refractory materials for aluminium reduction cells, *Light Metals* 1999, 231–238. https://doi.org/10.1007/978-3-319-48200-2_112
21. Ole-Jacob Siljan, Christian Schoning and Tor Grande, State-of-the-art alumino-silicate refractories for al electrolysis cells, *JOM* 1997, 295–301.
22. Kati Tschöpe, *Degradation of Cathode Lining in Hall-Héroult Cells*, PhD Thesis, Norwegian University of Science and Technology, 2010.
23. Samuel Senanu et al., Carbon cathode wear in aluminium electrolysis cells, *JOM* 2020, 72(1), 210–217. https://doi.org/10.1007/s11837-019-03717-z

24. Kristin Vasshaug et al., Wear of carbon cathodes in cryolite-alumina melts, *ECS Meeting Abstracts* 2007, 821–826. https://doi.org/10.1149/ma2006-02/45/2011
25. Shinjiro Toda and Tsutomu Wakasa, Improvement of abrasion resistance of graphitized cathode block for aluminium reduction cells, *Light Metals* 2003, 647–653.
26. Xian-an Liao and Harald A. Øye, Physical and chemical wear of carbon cathode materials, *Light Metals* 1998, 667–674, also in *Essential Readings in Light Metals* 2016, 984-991. https://doi.org/10.1007/978-3-319-48200-2_131
27. Siegfried Wilkening, Pierre Reny, Erosion rate testing of graphite cathode materials, *Light Metals* 2004, 597–602.
28. Kati Tschöpe et al., Critical reflections on laboratory wear tests for ranking commercial cathode materials in aluminium cells, *Light Metals* 2013, 1251–1256. https://doi.org/10.1002/9781118663189.ch211
29. R. C. Dorward, Reaction between aluminum and graphite in the presence of cryolite, *Metallurgical Transactions* 1973, 4(1), 386–388.
30. B. Novak et al., Fundamentals of aluminium carbide formation, *Light Metals* 2012, 1343–1348. https://doi.org/10.1007/978-3-319-48179-1_232
31. Samuel Senanu et al., Wetting of carbon cathodes by molten electrolyte and aluminium, *Light Metals* 2021, 699–707. https://doi.org/10.1007/978-3-030-65396-5_92
32. N. Eustathopoulos et al., The wetting of carbon by aluminium and aluminium alloys, *Journal of Materials Science* 1974, 9(8), 1233–1242. https://doi.org/10.1007/bf00551836
33. R. Ødegard, A. Sterten and J. Thonstad, On the solubility of aluminum in cryolitic melts, *Metallurgical Transactions B* 1988, 19(3), 449–457.
34. K. Vasshaug, *The influence of the formation and dissolution of aluminium carbide on the cathode wear in aluminium electrolysis cells*, PhD Thesis, Norwegian University of Science and Technology, 2008.
35. R. Keller, J. W. Burgman and P. J. Sides, Electrochemical reactions in the Hall-Héroult cathode, *Journal of Metals* 1987, 39(10), A43.
36. Alton T. Tabereaux et al., Erosion of cathode blocks in 180 kA prebake cells, *Light Metals* 1999, 187–192. https://doi.org/10.1007/978-3-319-48200-2_133
37. Pierre Reny and Siegfried Wilkening, Graphite cathode wear study at Alouette, *Light Metals* 2000, 399–404. https://doi.org/10.1007/978-3-319-48200-2_134
38. Pretesh Patel, Margaret Hyland and Frank Hiltmann, Influence of internal cathode structure on behavior during electrolysis Part II: porosity and wear mechanisms in graphitized cathode material, *Light Metals* 2005, 757–762. https://doi.org/10.1007/978-3-319-48200-2_136
39. Kati Tschöpe et al., Electrochemical wear of carbon cathodes in electrowinning of aluminum, *JOM* 2013, 65(11), 1403–1410. https://doi.org/10.1007/s11837-013-0605-4
40. H. Gudbrandsen, A. Sterten and R. Odegard, Cathodic dissolution of carbon in cryolitic melts, *Light Metals* 1992, 521–528.
41. Z. Wang et al., Cathode wear in electrowinning of aluminum investigated by a laboratory test cell, *Light Metals* 2016, 897–902. https://doi.org/10.1002/9781119274780.ch151
42. Bente M. Faaness et al., Ramming paste related failures in cathode linings, *Light Metals* 2016, 827–833. https://doi.org/10.1007/978-3-319-48200-2_109
43. Eirik Hagen, Mari-Ann Einarsrud and Tor Grande, Chemical stability of ceramic sidelinings in Hall-Héroult cells, *Light Metals* 2001, 257–263.
44. Zhaohui Wang, Aging of Si_3N_4-bonded SiC sidewall materials in Hall-Héroult cells, PhD Thesis, *Norwegian University of Science and Technology*, 2010.
45. Wei Gao, A. Hendry and G. Holling, Oxidation of nitride bonded silicon carbide in wet air atmosphere, *British Ceramic Transactions* 2002, 101(6), 231–236. https://doi.org/10.1179/096797802225004027
46. Egil Skybakmoen, Henrik Gudbrandsen and L.I. Stoen, Chemical resistance of sidelining materials based on sic and carbon in cryolitic melts - a laboratory study, *Light Metals* 1999, 215–222.

47. Ole-Jacob Siljan, Christian Schøning and Tor Grande, State-of-the-art alumino-silicate refractories for al electrolysis cells, *JOM* 2002, 54(5), 46–55. https://doi.org/10.1007/bf02701697
48. Ove Paulsen et al., Aging of insulating linings in aluminium electrolysis cells, *Light Metals* 2017, 551–559. https://doi.org/10.1007/978-3-319-51541-0_69
49. Raymond Luneng et al., Chemical stability of thermal insulating materials in sodium vapour environment, *Light Metals* 2017, 543–549. https://doi.org/10.1007/978-3-319-51541-0_68